Polarization measurements in a flow cytometer: Lissajous patterns in scatter plots of calibration beads

Doornbos, R.M.P.; Hoekstra, A.G.; Deurloo, K.E.I.; de Grooth, B.G.; Sloot, P.M.A.; Greve, J.

Publication date
1993

Published in
Cytometry

POLARIZATION MEASUREMENTS IN A FLOW CYTOMETER; LISSAJOUS PATTERNS IN SCATTER PLOTS OF CALIBRATION BEADS

RICHARD M.P. DOORNBOS, ALFONS G. HOEKSTRA, KIRSTEN E.J. DEURLOO°, BART G. DE GROOTH, PETER M.A. SLOOT°, and JAN GREV
APPLIED OPTICS GROUP, FACULTY OF APPLIED PHYSICS, UNIVERSITY OF TWENTE, THE NETHERLANDS
°PARALLEL SCIENTIFIC COMPUTING GROUP, FACULTY OF MATHEMATICS AND COMPUTER SCIENCE, UNIVERSITY OF AMSTERDAM, THE NETHERLAN

Poster; ISAC Colorado Springs
XVI Congress of the International Society for Analytical Cytology. ①
7 MAART, 21 - 26, 1993.
Abstract in Supplement 6, 1993 van Cytometry.

Introduction

Flow cytometric measurements of light scattering of 7 micrometer polystyrene calibration beads revealed remarkable Lissajous-like loops in two-parameter scatter plots. The signals in the orthogonal detectors show large fluctuations in these measurements and when non-conventional polarizations are used triangular and other forms appear in the scatterplots. The existence of such loops is shown to be in qualitative agreement with Lorenz-Mie theory of homogeneous spheres. The occurence of these patterns reflects the extreme size dependency of orthogonal light scattering of spheres.

Set-up

Our experimental flow cytometer consists of a 5 mW HeNe laser (632.8 nm); a 100 mm spherical lens to focus the light on the flow cell (see figure 1). Forward scattered light (2-6 degrees) is detected with a photodiode (PIN); the side scattered light is collected by a 0.4 NA objective, divided by a beam splitter and detected with two head-on photomultipliers. In the incident and the two orthogonal light paths the polarization can be changed by inserting either a quarter wave plate, a linear polarizer, or both. In figure 1 the set-up is prepared to measure S11+S12 and S11-S12 scattering matrix elements.

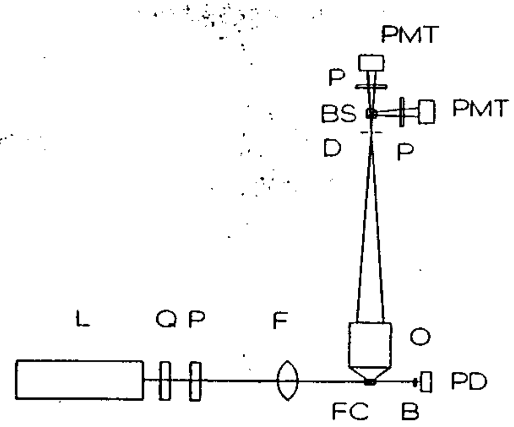

Figure 1
Set-up of polarization measurements in a flow cytometer.
L: laser; Q: quarter wave plate; P linear polarizer; F: focussing lens; FC: flow cell; B: beam dump; PD: photodiode; O: microscope objective; D: diaphragm; BS: beam splitter; PMT: photomultiplier.

Results

With a conventional set-up (vertical polarized incident light and total side scattering detected) we obtained the results shown in figure 2. The scatter plot (A) shows more or less a line instead of the expected round cluster. The histogram of the side scatter (B) shows an almost bimodal distribution. When non-conventional polarizations are used we obtained strange loops. In figure 3A we used +45 degrees polarized incident light and detected both horizontally and vertically polarized scattered light. We see a triangular form. In figure 3B we obtained with an other polarization combination (right circularly polarized light incident and +45 and -45 degrees polarized light detected) an "eight"-like pattern.

In figure 6A we gated the data in order to obtain corresponding forward scattering signals. Clearly the distribution in histogram B shows that particles with specific forward scattering signals appear in the chosen gates. This suggests that the particle size increases monotonous when rotating in one direction along the loop.

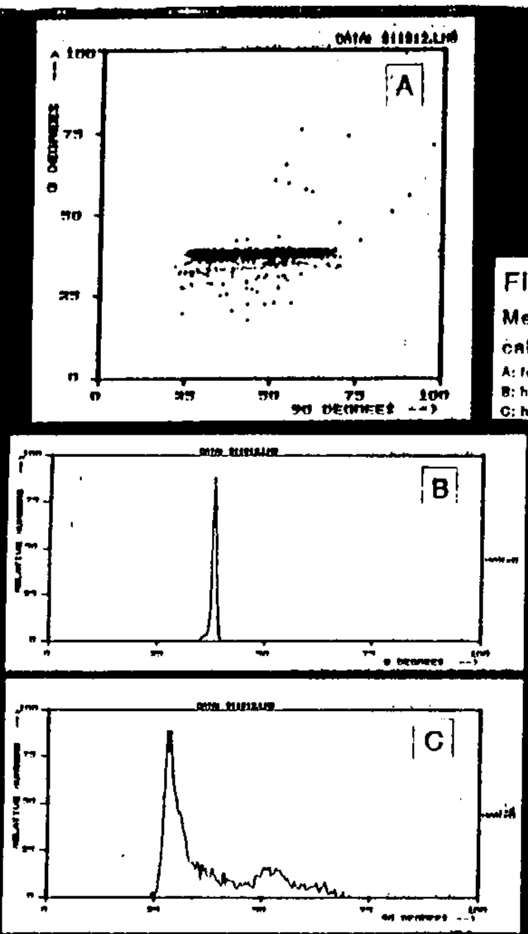

Figure 2
Measurement of 7 micrometer calibration beads
A: forward scatter versus side scatter
B: histogram of forward scatter
C: histogram of total side scatter

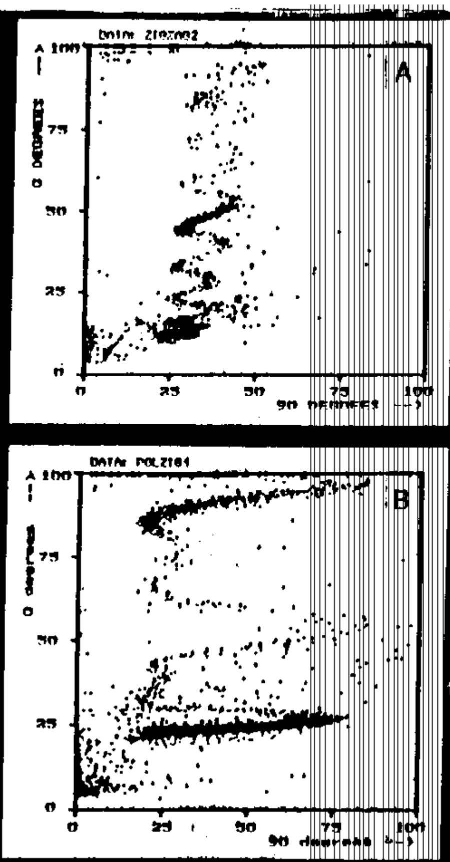

Figure 7
Forward versus side scattered light (488 nm) of 2.23 micrometer beads with (A) a large (0.4) and (B) a small numerical aperture (about 0.05).

②

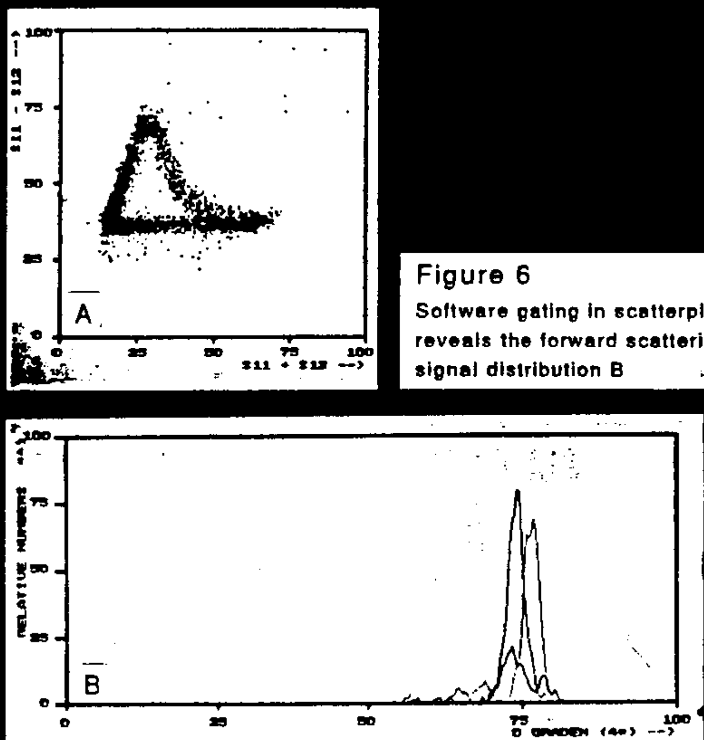

Figure 6
Software gating in scatterplot A reveals the forward scattering signal distribution B

Discussion

A possible explanation could be an extreme size dependency of the scattering signals. We see further a different behaviour with other detected polarizations. To find an explanation we tried to match the Lorenz-Mie theory for homogeneous spheres with our measurements. In figure 4 the calculated intensities of a 7 micrometer polystyrene bead are plotted as a function of the angle. Other polarizations show similar curves. The grey area indicates the region which is detected by the orthogonal detector. Increase of the bead size will shift the curve to the left side and the detected signal will change accordingly, as can be seen in figure 5. In this figure all non-zero integrated scattering matrix elements are plotted as a function of the size of the beads and the extreme size dependency is shown explicitly.

Using these calculations we can match our measurements as is shown in figure 3, where the dotted line indicates the theoretical scatter plot. The curve in figure 3A is one of the best agreements of theory and measurements we have obtained and this strongly supports our suggestion that the effects are due to Lorenz-Mie scattering. However, from figure 3B it is clear that still some differences remain unexplained.

Conclusions

We have shown that the Lissajous-like patterns can be described by Lorenz-Mie scattering, although some differences cannot be explained yet. The observed effects can be of importance to the interpretation of the measured CV of particles in the side scattering detector. It is therefore advisable to be careful to optimize the orthogonal light scattering by minimizing the CV.

148A

(3)

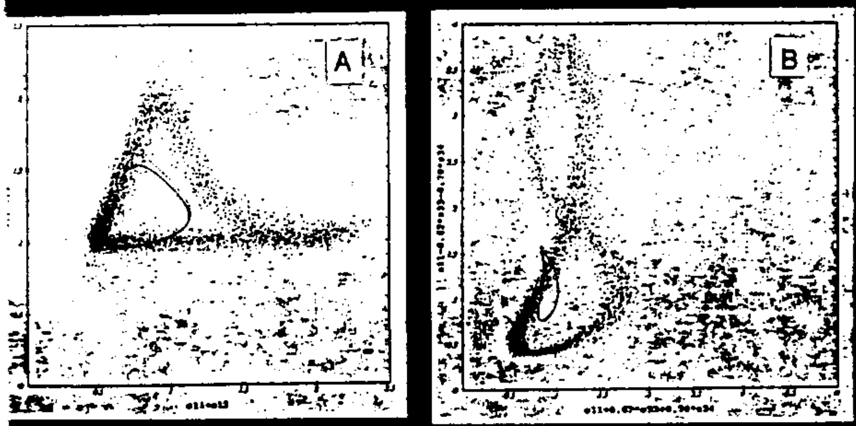

Figure 3
Measurement of 7 micrometer calibration beads
A: Incident polarization +45 degrees, detected polarization 0 and 90 degrees
B: Incident polarization right circular, detected polarization +45 and -45 degrees

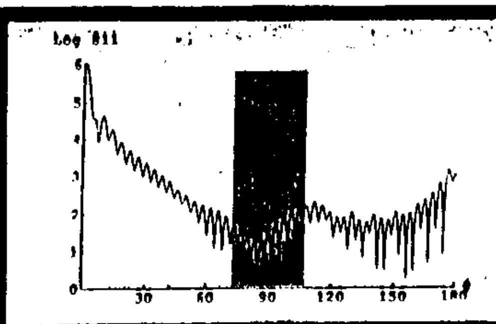

Figure 4
Angular dependence of scattering matrix element S11
(for 7.040 micrometer polystyrene beads; n=1.5874; wavelength 632.8 nm)

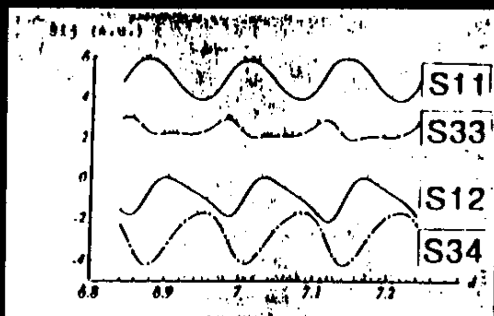

Figure 5
Integrated matrix elements sij as a function of the bead size
(numerical aperture 0.4)